

Controlling the Rigidity of Kinesin-Propelled Microtubules in an *In Vitro* Gliding Assay Using the Deep-Sea Osmolyte Trimethylamine *N*-Oxide

Arif Md. Rashedul Kabir,^{*,∇} Tasrina Munmun,[∇] Tomohiko Hayashi, Satoshi Yasuda, Atsushi P. Kimura, Masahiro Kinoshita, Takeshi Murata, Kazuki Sada, and Akira Kakugo^{*}



Cite This: *ACS Omega* 2022, 7, 3796–3803



Read Online

ACCESS |



Metrics & More

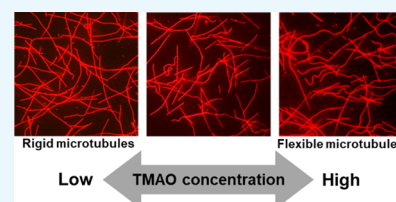


Article Recommendations



Supporting Information

ABSTRACT: The biomolecular motor protein kinesin and its associated filamentous protein microtubule have been finding important nanotechnological applications in the recent years. Rigidity of the microtubules, which are propelled by kinesin motors in an *in vitro* gliding assay, is an important metric that determines the success of utilization of microtubules and kinesins in various applications, such as transportation, sensing, sorting, molecular robotics, etc. Therefore, regulating the rigidity of kinesin-propelled microtubules has been critical. In this work, we report a simple strategy to regulate the rigidity of kinesin-propelled microtubules in an *in vitro* gliding assay. We demonstrate that rigidity of the microtubules, propelled by kinesins in an *in vitro* gliding assay, can be modulated simply by using the natural osmolyte trimethylamine *N*-oxide (TMAO). By varying the concentration of TMAO in the gliding assay, the rigidity of microtubules can be modulated over a wide range. Based on this strategy, we are able to reduce the persistence length of microtubules, a measure of microtubule rigidity, ~ 8 fold by using TMAO at the concentration of 1.5 M. Furthermore, we found that the decreased rigidity of the kinesin-propelled microtubules can be restored upon elimination of TMAO from the *in vitro* gliding assay. Alteration in the rigidity of microtubules is accounted for by the non-uniformity of the force applied by kinesins along the microtubules in the presence of TMAO. This work offers a facile strategy to reversibly regulate the rigidity of kinesin-propelled microtubules *in situ*, which would widen the applications of the biomolecular motor kinesin and its associated protein microtubule in various fields.



INTRODUCTION

According to the prevailing view, the biomolecular motor protein kinesin is the smallest natural machine that, in cooperation with its associated filamentous protein microtubule (MT), can convert the energy obtained from hydrolysis of adenosine triphosphate (ATP) into mechanical work with a remarkably high efficiency and specific power.^{1,2} Nanometer scales, engineering properties, and natural abundance of kinesins and MTs have been the motivations to utilize the biomolecular motor system as the building block, actuator, and sensor in hybrid micro- or nanodevices.^{3–5} *In vitro* gliding assay, where MTs are propelled by kinesins adsorbed to a substrate in the presence of ATP, has revolutionized the applications of MTs and kinesins in synthetic environments for nanotransportation and nanostructuring,^{6,7} surface imaging,⁸ characterizing the surface mechanical deformation,⁹ force measurement,¹⁰ swarm robotics,¹¹ molecular computing,^{12,13} and fabrication of artificial muscles.¹⁴ Rigidity of the kinesin-propelled MTs plays a crucial role in successful accomplishment of these tasks. For example, in molecular transportation, rigidity of the kinesin-propelled MTs affects the direction of the shuttles and delivery destination of cargo materials;¹⁵ in molecular robotics, the dynamic behavior and swarm pattern of the robots depend on the rigidity of the MTs;¹⁶ in active self-assembly, morphologies of the self-assembled structures are

determined by the rigidity of the MTs.^{17,18} Therefore, it has been inevitable to control the rigidity of MTs, which in turn would permit controlling the applications of MTs. In the previous attempts, rigidity of MTs was tuned by engineering their electrical properties or by changing the nucleotide used for polymerization of tubulin proteins into MTs.¹⁵ Such manipulations required tuning of tubulin polymerization conditions or conjugation of DNA, peptides to MTs, or the presence of MT-associated proteins (MAPs) or MT stabilizers.^{15,19–21} While these methods were useful in tuning the rigidity of MTs, eventually, the structure of MTs was permanently affected, which restricted reversible regulation of the MT rigidity. In the present work, we demonstrate that rigidity of the MTs, propelled by kinesins in an *in vitro* gliding assay, can be regulated *in situ* by using trimethylamine *N*-oxide (TMAO). TMAO is an osmolyte found in deep-sea animals and is known to stabilize proteins under stressful or denaturing

Received: November 26, 2021

Accepted: January 5, 2022

Published: January 24, 2022



conditions of heat, pressure, and chemicals.^{22–25} Based on our results we confirm that, without depending on any prior modification of MTs, rigidity of the MTs translocating on a kinesin-coated substrate can be reduced by using TMAO. The extent of decrease in the rigidity of the gliding MTs is found to be dependent on the concentration of TMAO employed. Importantly, upon elimination of TMAO, the rigidity of MTs can be restored, which facilitates a simple means for *in situ* reversible regulation of the rigidity of kinesin-propelled MTs in a gliding assay. Such an ability to reversibly regulate the rigidity of kinesin-propelled MTs would contribute in widening the applications of the biomolecular motors in nanotechnology, material science, and bioengineering.

RESULTS AND DISCUSSION

We have explored the utility of TMAO in controlling the rigidity of kinesin-propelled MTs by performing an *in vitro* gliding assay of MTs on a kinesin-coated substrate (Figure 1),

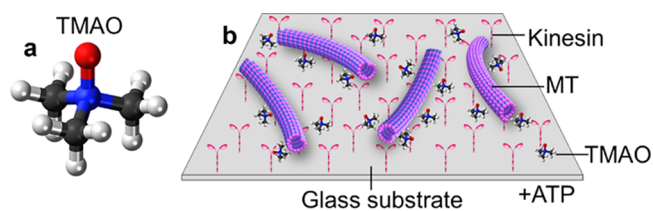


Figure 1. Schematic representation of the (a) molecular structure of TMAO and (b) *in vitro* gliding assay of MTs on a kinesin-coated glass substrate in the presence of TMAO. In the molecular structure of TMAO, the red, blue, black, and white spheres denote the oxygen, nitrogen, carbon, and hydrogen atoms, respectively. “+ATP” indicates the presence of ATP in the *in vitro* gliding assay.

where the concentration of TMAO was varied between 0 and 1500 mM. This range of TMAO concentration was selected based on a previous report in which detachment of MTs from the kinesin-coated substrate was observed for the TMAO concentrations higher than 1500 mM.²⁵ Despite the presence of TMAO in the gliding assay, MTs exhibited translational motion on the kinesin-coated substrate. The velocity of MTs decreased gradually upon increasing the concentration of TMAO, which agrees to previous reports^{25,26} (Figure S1). The observed decrease in velocity of MTs upon increasing the TMAO concentration indicates suppression of kinesins’ activity by TMAO akin to that reported for the case of the actin–myosin system.²⁷

We noticed that the conformation of the gliding MTs was changed with time from a straight/linear to a bent or buckled state when the concentration of TMAO was relatively high, e.g., 1200 mM (Figure S2). Such a change in MT conformation was not noticed in the absence of TMAO or in the presence of TMAO of low concentrations, e.g., 200 mM (Figure S2). Based on this observation, we particularly focused on the conformation of MTs after 30 min of initiating the gliding assay. As shown in Figure 2, conformation of the gliding MTs was substantially changed upon increasing the concentration of TMAO in the gliding assay. The gliding MTs mostly retained their straight or linear conformation in the absence of TMAO (Movie S1) or in the presence of relatively low TMAO concentrations (e.g., 400 mM). Upon increasing the TMAO concentration further (e.g., 1000 mM), considerable bending and local buckling of the gliding MTs were observed (Figure 2 and Movie S2). Further increase in the

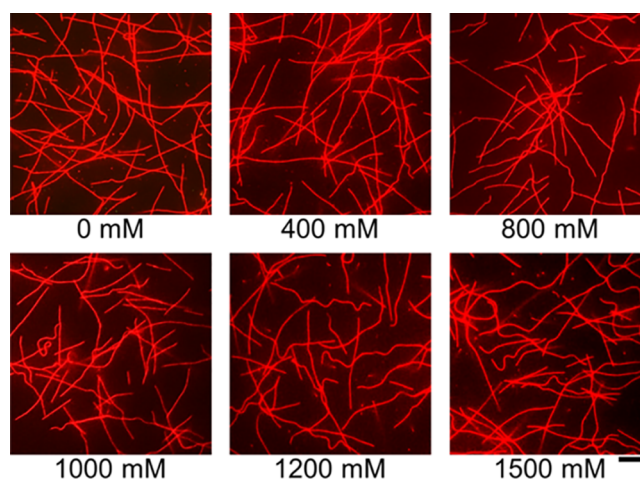


Figure 2. Fluorescence microscopy images show the effect of TMAO on the conformation of the MTs gliding on a kinesin-coated substrate. The concentration of TMAO in each case is provided below the respective images. The images were captured after 30 min of initiation of the gliding assay. Scale bar: 5 μm .

TMAO concentration to 1200 or 1500 mM resulted in extensive bending or buckling of the gliding MTs (Movie S3), which agrees to a recent report where gliding MTs were reported to follow spiral trajectories in the presence of relatively high TMAO concentrations.²⁸ Thus, from these results, it is evident that the conformation of the gliding MTs was gradually changed from a “straight” to a “curved” or “bent” state upon increasing the concentration of TMAO in the gliding assay.

To confirm the changes in MT conformation in the presence of TMAO, we analyzed the end-to-end length and contour length of the MTs under the conditions discussed above (Figure S3). The results clearly reveal that in the absence of TMAO or in the presence of TMAO of relatively low concentrations, the end-to-end length of MTs was very close to their contour length, which indicates the straight conformation of the MTs. However, upon increasing the concentration of TMAO, particularly close to or above 1000 mM, the end-to-end length of MTs became much shorter than their corresponding contour lengths. This decrease in the end-to-end length confirms the change in conformation of MTs from the straight to the curved or bent state. These results imply that, in an *in vitro* gliding assay, the kinesin-propelled MTs became flexible in the presence of TMAO. We have quantified the effect of TMAO on the rigidity of MTs by estimating the persistence length of the MTs, which is considered as a measure of their rigidity. The persistence length was estimated from the fitting of the squared end-to-end length of the MTs against their contour length (Figure 3). The outcome, shown in Figure 4a, clearly reveals that the persistence length of MTs gradually decreased upon increasing the concentration of TMAO in the *in vitro* gliding assay. The persistence length of MTs was $285 \pm 47 \mu\text{m}$ (fit value \pm standard deviation) in the absence of TMAO, which agrees to that previously reported in the literature.^{16,29} At the highest concentration of TMAO employed in this study (1.5 M), the persistence length of MTs decreased to $37 \pm 4 \mu\text{m}$. Based on the above results, it is evident that the rigidity of the MTs, propelled by kinesins in an *in vitro* gliding assay, can be modulated by tuning the concentration of TMAO in the gliding assay. To understand

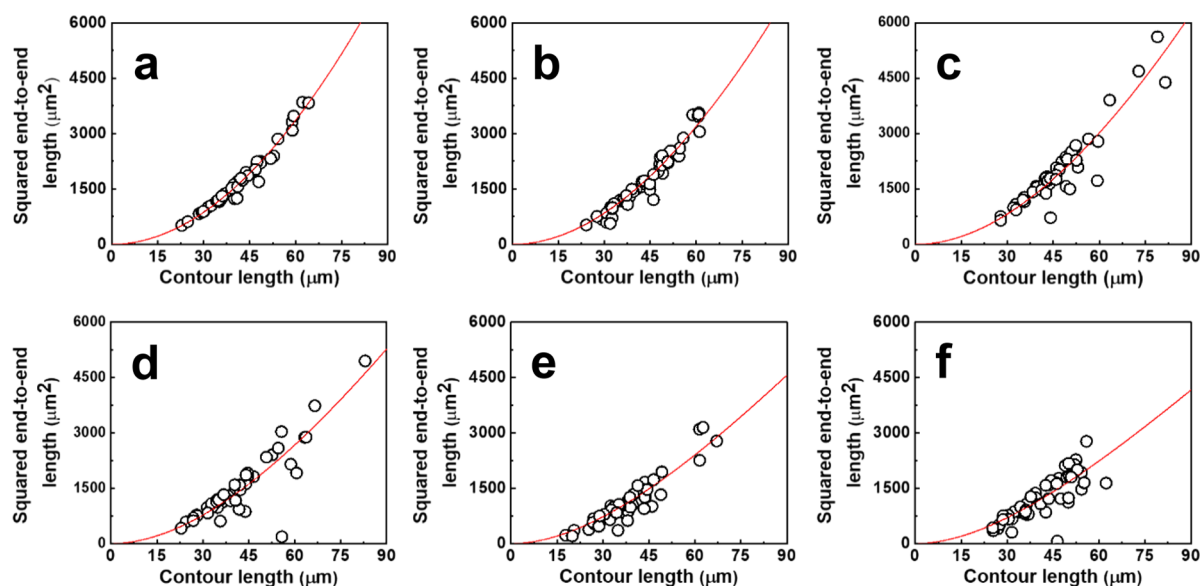


Figure 3. Estimation of the persistence length of kinesin-propelled MTs in the presence of TMAO of various concentrations: (a) 0 mM, (b) 400 mM, (c) 800 mM, (d) 1000 mM, (e) 1200 mM, and (f) 1500 mM. The red solid lines indicate fitting of the data according to the equation provided in the [Experimental Section](#).

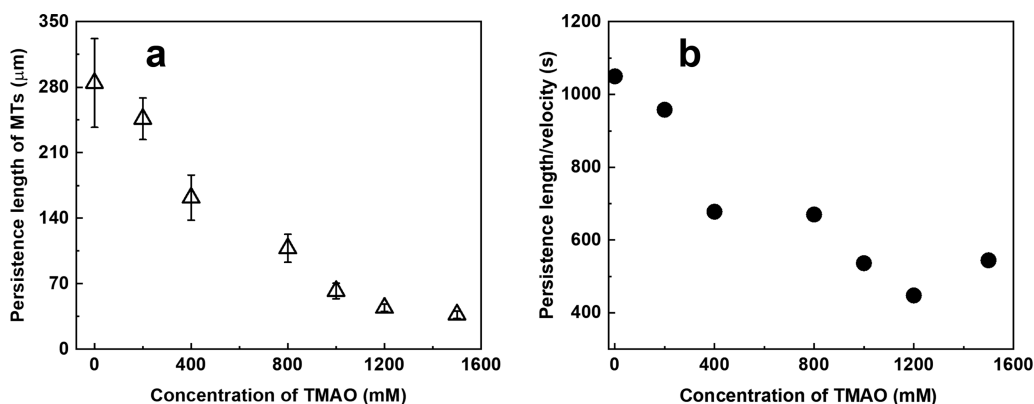


Figure 4. (a) Change in the persistence length of MTs, in an *in vitro* gliding assay, upon increasing the concentration of TMAO in the gliding assay from 0 to 1500 mM. Error bar: standard deviation. (b) Persistence length of MTs/velocity of MTs as a function of varying concentration of TMAO.

if such changes in the persistence length of MTs is related to the change in MT velocity or not, we divided the persistent length of MTs by the average MT velocity and plotted against the TMAO concentration in each case ([Figure 4b](#)). The result revealed that the persistence length changed non-linearly with the MT velocity. Thus, the gradual decrease in MT rigidity, i.e., the persistence length, in the presence of TMAO, does not seem to be the result of the decreased MT velocity upon increasing the TMAO concentration in the gliding assay.

Next, we have sought to know whether the change in rigidity of MTs in the gliding assay, caused by TMAO, is permanent or not. To investigate, first, we demonstrated *in vitro* gliding assay of MTs on kinesins in the absence of TMAO; then, we applied 1200 mM TMAO in the flow cell by mixing with the ATP buffer ([Figure 5](#)). As discussed above, the gliding MTs became curved or bent upon application of TMAO. We then eliminated the TMAO from the gliding assay by extensive washing of the flow cell with ATP buffer where TMAO was absent. The curved gliding MTs regained their straight conformation upon elimination of the TMAO from the flow cell ([Figure 5](#)). Initially, the persistence length of MTs was 278

$\pm 42 \mu\text{m}$, which decreased to $75 \pm 11 \mu\text{m}$ in the presence of 1200 mM TMAO. The persistence length of MTs was restored to $262 \pm 27 \mu\text{m}$ upon elimination of the TMAO ([Figure 5](#)). This is to note that, in these experiments, velocity of MTs was $293 \pm 31 \text{ nm/s}$ in the absence of TMAO, which decreased to $105 \pm 19 \text{ nm/s}$ in the presence of 1200 mM TMAO. Upon elimination of the TMAO, the velocity of MTs was restored to $289 \pm 36 \text{ nm/s}$, which indicates that the kinesins regained their activity after washing out TMAO. Overall, the above results confirm that the change in rigidity of the kinesin-propelled MTs, in the presence of TMAO, is not permanent and TMAO offers a useful means to modulate the rigidity of gliding MTs in a reversible manner.

To understand the mechanism behind change in the rigidity of the kinesin-propelled MTs in the presence of TMAO, we investigated the role of various relevant factors such as viscosity of medium, velocity of MTs, and activity of kinesins in alteration of the persistence length of MTs in an *in vitro* gliding assay. Since the viscosity of TMAO solution is higher than that of water,³⁰ one may suspect that the decrease in the persistence length of kinesin-propelled MTs in the presence of TMAO

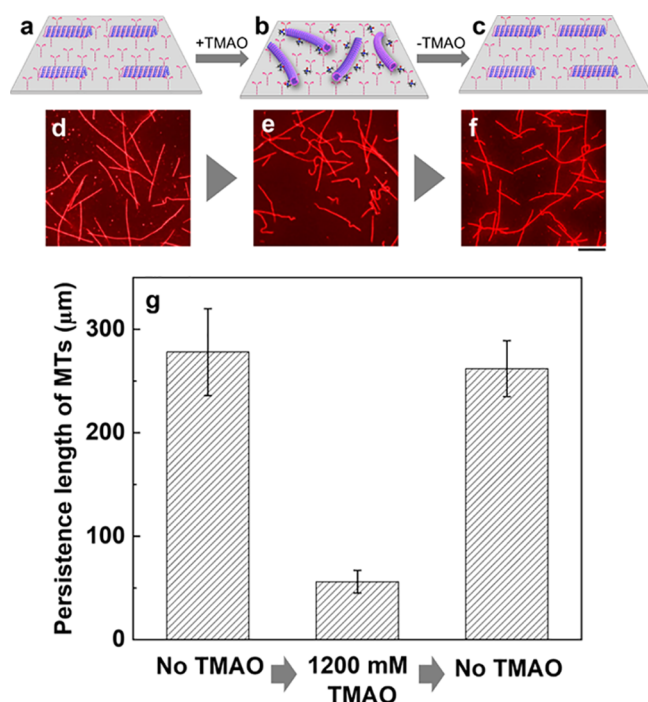


Figure 5. (a–c) Schematic representation of the experimental design used to demonstrate reversible regulation of the persistence length of kinesin-driven MTs, in an *in vitro* gliding assay, using TMAO. Initially, the gliding assay of MTs was performed in the absence of TMAO (a), which was followed by addition of 1200 mM TMAO in the gliding assay (b). Finally, the flow cell was washed to eliminate the TMAO from the gliding assay (c). Here, “+TMAO” and “–TMAO” indicate addition and elimination of TMAO to and from the gliding assay, respectively. (d–f) Fluorescence microscopy images confirm reversible change in conformation of the MTs using TMAO. MTs were of straight or linear conformation before the addition of TMAO in the gliding assay (d). In the presence of TMAO in the gliding assay, the MTs became curved (e). Upon washing out of the TMAO from the flow cell, the MTs regained their straight conformation (f). (g) Persistence length of the kinesin-propelled MTs before the addition of TMAO, in the presence of 1200 mM TMAO and after elimination of the TMAO. Scale bar: 20 μm , error bar: standard deviation.

might be related to the increased viscosity of the medium. Therefore, we explored the effect of viscosity of the medium on the persistence length of kinesin-propelled MTs by performing *in vitro* gliding assay in the presence of 25% (w/v) ethylene glycol (EG), glycerol, and bovine serum albumin (BSA). The molar concentrations of 25% (w/v) EG, glycerol, and BSA solutions were 4.03, 2.71, and 0.004 M, respectively. According to the published data, viscosities of the 25% (w/v) EG, glycerol, and BSA solutions are 2.0, 2.1, and 5.9 mPa·S, respectively, at 20 °C.³⁰ The results obtained from the gliding assay using the viscous agents revealed no substantial difference in the persistence length of the motile MTs despite the presence of the EG, glycerol, and BSA (Figures S4 and S5). Thus, it appears that the persistence length of the kinesin-propelled MTs is not dependent on the viscosity of the medium. Therefore, based on these results, it can be concluded that the observed decrease in the persistence length of kinesin-propelled MTs in the presence of TMAO is not the result of increased viscosity of the medium due to the presence of TMAO.

We then investigated whether the change in rigidity of MTs is triggered by the reduction in the velocity of kinesin-

propelled MTs due to the presence of TMAO. We performed gliding assay of MTs by decreasing the fuel (ATP) concentration in the absence of TMAO. Upon decreasing the concentration of ATP from 5 mM to 25, 10, and 5 μM , the velocity of MTs became 93 ± 4 nm/s (average \pm standard deviation), 41 ± 7 nm/s, and 22 ± 5 nm/s, respectively (sample number, $n = 40$). It is to note that, at the saturating ATP concentration (5 mM), the velocity of MTs was 252 ± 30 nm/s in the absence of TMAO and 99 ± 17 nm/s and 68 ± 12 nm/s in the presence of 1200 and 1500 mM TMAO, respectively. Despite the reduction in MT velocity upon decreasing the fuel concentration in the absence of TMAO, the straight conformation of the gliding MTs was maintained (Figure 6). In the Figure 6, we summarize the changes in velocity of MTs upon changing the ATP concentration in the absence of TMAO and the persistence length of MTs under each condition. From these results, it is evident that the velocity of the MTs has no effect on their persistence length. Thus, the decrease in rigidity or persistence length of the motile MTs in the presence of TMAO is not the result of the reduced MT velocity, but rather it seems to be the result of the presence of TMAO in the gliding assay system.

We have also investigated whether TMAO alone can directly affect the rigidity of the MTs or not. We monitored the conformation of MTs on a kinesin-coated substrate in the presence of 1200 mM TMAO but in the absence of ATP. We found that even though a high concentration of TMAO was present, the straight conformation of the immotile MTs was not changed to a curved or buckled state (Figure S6). Furthermore, instead of attaching the MTs on a kinesin-coated surface, we mixed the solutions of MTs and TMAO (1200 mM) in the absence of kinesin and ATP. As shown by the fluorescence microscopy images in Figure S7, bending or buckling of the MTs, suspended in bulk solution, was not observed even though TMAO was present at a high concentration. Based on these results, it can be concluded that TMAO solely is not responsible for altering the conformation of MTs in the gliding assay from a linear to a bent or buckled state. Furthermore, a dynamic condition, i.e., motility of the MTs on kinesins is a prerequisite for modulating the conformation or rigidity of the MTs using TMAO. TMAO is known to stabilize motor proteins, e.g., myosin or kinesin and suppress their activity.^{24–27} In the previously published reports, it was suspected that TMAO may suppress the rate-limiting step of biomolecular motors during their mechano-chemical cycle of ATPase activity in the presence of their associated protein filaments.²⁷ The conformational change of motor heads during the rate-limiting step of ATPase cycle may not readily take place in the presence of TMAO. Consequently, bending or buckling of motor-driven protein filaments (actin–myosin) was observed in the presence of TMAO.²⁷ Taken together with the suppressed activity of kinesins by TMAO,^{25,26} the bent or buckled conformation of motile MTs, as observed in this work, indicates that TMAO may have a similar effect on the ATPase cycle of kinesins. In that case, possible retardation of the force-generating step of kinesins is likely to subside the uniformity of the driving force within single MT filaments resulting in the deformation, i.e., bending or buckling of the MT filaments.

We have verified this hypothesis about the involvement of non-uniform driving force of kinesins along gliding MT filaments in the deformation of the MTs. We performed gliding assay of MTs on a substrate, which was coated by two

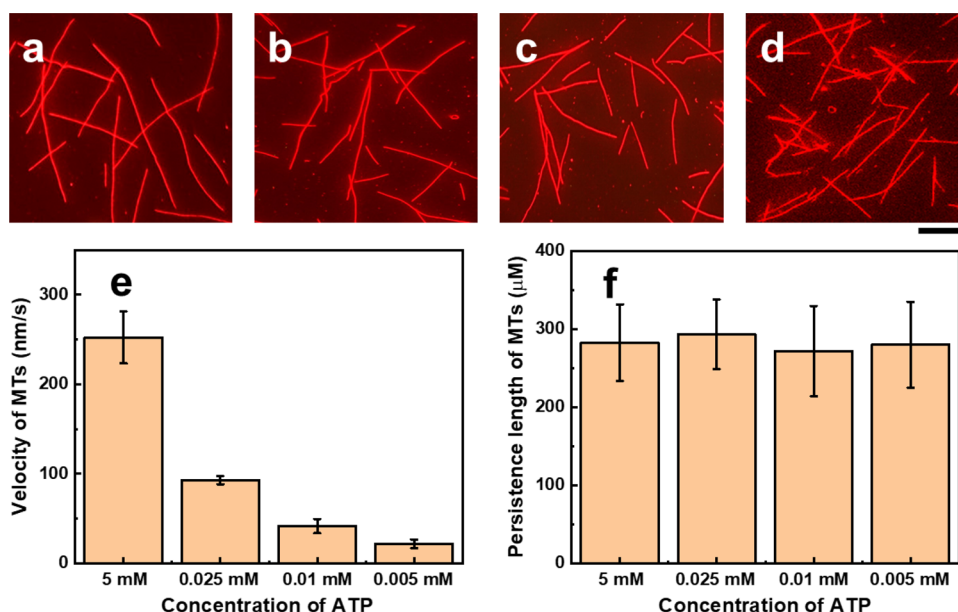


Figure 6. Effect of ATP concentration on the conformation, velocity, and persistence length of MTs. Fluorescence microscopy images show MTs on a kinesin-coated substrate in the presence of (a) 5 mM, (b) 0.025 mM, (c) 0.01 mM, and (d) 0.005 mM ATP. In all the cases, the straight/linear conformation of the MTs was retained. (e) Change in the velocity of MTs upon changing the ATP concentration in the gliding assay on a kinesin-coated substrate. (f) Persistence length of gliding MTs at various ATP concentrations. Despite the decrease in MT velocity due to the decrease in the ATP concentration in the gliding assay, the persistence length of MTs was not changed noticeably. Error bar: standard deviation. Scale bar: 10 μm .

types of kinesins where one type was much faster than the other one. In the gliding assay, the velocity of the MTs propelled by the fast kinesin was much higher ($\sim 242 \pm 32$ nm/s) compared to that propelled by the slow kinesin (8 ± 2 nm/s) although the in-feed concentration of both the kinesin was the same (800 nM). When the slow and the fast kinesins were adsorbed to a substrate at a surface density ratio of 4:1, the gliding MTs were found to undergo bending or buckling (Movie S4). Along with such deformation, MTs were found to change their gliding direction abruptly when the surface density ratio of the slower kinesin to the faster kinesin was 1:2 (Movie S5). Such deformation of gliding MTs was not observed when MTs were propelled by only the fast kinesin (Movie S6). Such deformation of the MTs, concurrently propelled by the fast and slow kinesin, could be accounted for by the following mechanism.³¹ MT filaments transiting from a track of slow kinesins to a track of fast kinesins will experience tensile forces, whereas filaments transiting from a track of fast kinesins to a track of slow kinesins will be under compression, which may result in bending or buckling of the MTs. Due to the higher density of the slow kinesin on the assay substrate compared to the fast kinesin (Movie S4), bending of MTs was the dominant phenomenon. When an MT was propelled by both the fast and the slow kinesins at the same time, a non-uniform force that originated from the kinesins worked along the MT. The buckling and abrupt change in gliding direction of the MTs were the results of such non-uniform force applied by the kinesins to the MTs. These results confirm that disrupted uniformity of kinesins' force along MTs can give rise to deformation of MTs in the form of bending or buckling. Thus, the bending deformation or buckling, as well as the change in rigidity of the gliding MTs, as observed in our work in the presence of TMAO, appears to be the result of TMAO-mediated disruption of the uniformity in the force generated by the kinesins. It is not the suppression of kinesins' activity,

but rather it is the non-uniform force generated by the kinesins in the presence of TMAO, which seems to be responsible for the change in rigidity or persistence length of MTs in the presence of TMAO. Systematic studies will be performed in the future to explore in detail the underlying mechanism behind the change in MT rigidity of kinesin-propelled MTs in the presence of TMAO.

This is to note that the persistence length of the kinesin-propelled MTs, estimated in this work in the absence of TMAO, agrees well to our previous report.¹⁶ However, the MT persistence length estimated in this study is smaller compared to the values reported in the literature.³² In the past, numerous attempts were devoted to measure the persistence length or rigidity of MTs based on diverse experimental strategies.³³ The reported values of MT rigidity varied significantly due to the difference in the experimental design. The rigidity of MTs is known to depend also on the MT polymerization conditions, MT-associated proteins, post-translational modification state of tubulins, etc.³³ According to a previous report, kinesin works as a softening agent for MTs.³⁴ Thus, the difference in the experimental design and presence of kinesin seem to be the reasons behind the smaller persistence length of MTs estimated in this work compared to that reported in the literature.³²

CONCLUSIONS

We report a facile strategy to reversibly regulate the rigidity of MTs *in situ*, in an *in vitro* gliding assay, by using the deep-sea osmolyte TMAO. Unlike the previous works, the presented method does not require any prior and permanent modification of the MTs to regulate their rigidity in the gliding assay. The non-uniform driving force generated by the kinesins, mediated by TMAO, is found to alter the rigidity and conformation of the gliding MTs. According to the literature, TMAO is known for stabilizing proteins in living organ-

isms.^{35,36} Particularly, the presence of TMAO in living organisms at very high concentrations (at the mM level) has been confirmed^{37,38} that plays crucial roles in protecting proteins from various denaturing stress. In recent years, TMAO has also attracted much attention for stabilizing the biomolecular motor kinesin and its associated filamentous protein MT in synthetic environments.^{24,25,30} Therefore, it is intriguing to explore the effect of TMAO on the activity and relevant features of the most widely studied biomolecular motor system, kinesin-MTs. *In vitro* gliding assay has been a useful platform for studying the biophysical and chemomechanical aspects of biomolecular motors and their associated protein filaments. Moreover, *in vitro* gliding assay serves as the basis for many applications of biomolecular motors, such as nanoscale transportation, sensing, sorting, self-assembly, molecular computation, robotics, etc.^{39,12} Therefore, introduction of TMAO in the gliding assay of MTs on kinesins, as demonstrated in this work, will contribute to further advance the applications of MTs/kinesins in nanotechnology, materials science, and bioengineering. On the other hand, this work will help enrich our knowledge on the physiological significance of TMAO in relation to the functions of biomolecular motors and should encourage future investigations in order to unveil the effect of TMAO on the stability, mechanical property, and other physiological aspects of cytoskeletal proteins and associated biomolecular motors. Such outcomes would be of great physiological significance.⁴⁰

■ EXPERIMENTAL SECTION

Chemicals and Buffers. TMAO was purchased from Sigma-Aldrich and used without further purification. BRB80 buffer was prepared, maintaining the final concentrations of 80 mM PIPES, 1 mM MgCl₂, and 1 mM EGTA. The pH of the BRB80 buffer was adjusted to 6.8 using KOH. TMAO solution was prepared by dissolving the purchased TMAO in BRB80 buffer. The BRB80-TMAO imaging solutions contained 5 mM ATP, 1 mM DTT, 2 mM trolox, 1 mM MgCl₂, 10 μM taxol, 0.5 mg mL⁻¹ casein, 4.5 mg mL⁻¹, D-glucose, 50 U mL⁻¹ glucose oxidase, and 50 U mL⁻¹ catalase.

Purification and Labeling of Tubulin and Preparation of MTs. Tubulin was purified from fresh porcine brain using a high-concentration PIPES buffer (1 M PIPES, 20 mM EGTA, 10 mM MgCl₂; pH adjusted to 6.8 using KOH) according to a previous report.⁴¹ Atto550-labeled tubulin (RT) was prepared using Atto550 NHS ester (ATTO-TEC, GmbH) according to a standard technique.⁴² The labeling ratio of fluorescence dye to tubulin was ~1.0 as determined from the absorbance of tubulin at 280 nm and fluorescence dye at 554 nm. MTs were prepared by polymerizing a mixture of RT and non-labeled tubulin (WT) (RT:WT = 1:1; final tubulin concentration = 40 μM). Then, 4.0 μL of a mixture of RT and WT was mixed with 1 μL of GTP-premix (5 mM GTP, 20 mM MgCl₂, 25% DMSO in BRB80) and incubated at 37 °C for 30 min. The MTs were stabilized using paclitaxel after polymerization (50 μM paclitaxel in DMSO).

Expression and Purification of Kinesin. GFP-fused recombinant kinesin-1 construct consisting of the first 465 amino acid residue of human kinesin-1 (K465-GFP-avitag) with an N-terminal histidine tag and a C-terminal avidin-tag was used to propel MTs in an *in vitro* gliding assay. The expression and purification of the kinesin were done as described in a previously published report.⁴³

***In Vitro* Gliding Assay.** A flow cell with dimensions of 9 × 2 × 0.1 mm³ (*L* × *W* × *H*) was assembled from two cover glasses of sizes (9 × 18) mm² and (40 × 50) mm² (MATSUNAMI) using a double-sided tape as a spacer. First, the flow cell was filled with 5 μL of 1 mg mL⁻¹ streptavidin solution (Sigma-Aldrich, S4762) and incubated for 5 min. The flow cell was then washed with wash buffer (80 mM PIPES, 1 mM EGTA, 1 mM MgCl₂, and ~0.5 mg mL⁻¹ casein; pH 6.8). Next, 5 μL of K465-GFP-avitag solution (800 nM) was introduced into the streptavidin-coated flow cell. The flow cell was then incubated for 5 min to allow binding of kinesins to the glass surface through interaction with the streptavidin. After washing the flow cell with 10 μL of wash buffer, 10 μL of MT solution (200 nM, paclitaxel-stabilized GTP-MTs) was introduced and incubated for 5 min, which was followed by washing with 10 μL of wash buffer. Finally, motility of MTs was initiated by applying 5 μL of motility buffer containing 5 mM ATP. In the case of the experiments where TMAO was used, 5 μL of motility buffer containing 5 mM ATP and TMAO of prescribed concentrations was infused into the flow cell. The MTs were then monitored using a fluorescence microscope. For the *in vitro* gliding assay, using a combination of a fast kinesin and a slow kinesin, a mixture of the fast and slow kinesin was applied to the flow cell after application of streptavidin solution. In the mixture, the molar ratios of the slow kinesin to the fast kinesin were 4:1 and 1:2 in two different gliding assay experiments. All other steps were the same to that described above. All the above experiments were performed at room temperature (~22–25 °C).

Microscopy Image Capture and Data Analysis.

Samples were illuminated with a 100 W mercury lamp and visualized by an epi-fluorescence microscope (Eclipse Ti; Nikon) equipped with an oil-coupled Plan Apo 60 × 1.40 objective (Nikon). A filter block with UV-cut specification (TRITC: EX540/25, DM565, BA606/55; Nikon) was used in the optical path of the microscope that allowed visualization of MTs after eliminating the UV part of radiation and minimized the harmful effect of UV radiation on samples. Images were captured using a cooled CMOS camera (Neo CMOS; Andor) connected to a PC. To capture images of MTs for several minutes, ND4 filters (25% transmittance) were inserted into the illuminating light path of the fluorescence microscope to avoid photobleaching. The images or movies captured under the epi-fluorescence microscope were analyzed using image analysis software (ImageJ 1.46r).

Estimation of the Persistence Length of MTs. In order to estimate the persistence length of MTs, we measured the end-to-end length and contour length of the MTs at various TMAO concentrations (from 0 to 1500 mM). The persistence length of MTs was then estimated from the fitting of the “squared end-to-end length” of MTs against their corresponding “contour length” according to the following equation:^{44,45}

$$R^2 = 2L_p^2 \left[\left(\frac{L}{L_p} - 1 \right) + \exp\left(\frac{-L}{L_p} \right) \right]$$

Here, *R* is the end-to-end length, *L* is the contour length, and *L_p* is the persistence length of MTs.

■ ASSOCIATED CONTENT

Supporting Information

The Supporting Information is available free of charge at <https://pubs.acs.org/doi/10.1021/acsomega.1c06699>.

Additional experimental results on the effect of TMAO on velocity of kinesin-propelled MTs, time-lapse images of kinesin-propelled MTs in the absence and in the presence of TMAO; end-to-end length and contour length of MTs under various conditions; images of MTs propelled by kinesins in the presence of ethylene glycol, glycerol, and bovine serum albumin; images of MTs in the absence of ATP but in the presence/absence of TMAO in the gliding assay; images of MTs in the presence/absence of TMAO in bulk; and captions for supporting movies (PDF)

In vitro gliding assay of MTs on kinesins in the absence of TMAO (MP4)

In vitro gliding assay of MTs on kinesins in the presence of 1000 mM TMAO (MP4)

In vitro gliding assay of MTs on kinesins in the presence of 1500 mM TMAO (MP4)

In vitro gliding assay of MTs on a substrate coated with both the fast and slow kinesin (AVI)

Abrupt change in the gliding direction of a MT in an *in vitro* gliding assay performed on a substrate coated with both the fast and slow kinesin (AVI)

In vitro gliding assay of MTs on the fast kinesin (AVI)

AUTHOR INFORMATION

Corresponding Authors

Arif Md. Rashedul Kabir – Faculty of Science, Hokkaido University, Sapporo 060-0810, Japan; orcid.org/0000-0001-6367-7690; Email: kabir@sci.hokudai.ac.jp

Akira Kakugo – Faculty of Science and Graduate School of Chemical Sciences and Engineering, Hokkaido University, Sapporo 060-0810, Japan; orcid.org/0000-0002-1591-867X; Email: kakugo@sci.hokudai.ac.jp

Authors

Tasrina Munmun – Graduate School of Chemical Sciences and Engineering, Hokkaido University, Sapporo 060-0810, Japan

Tomohiko Hayashi – Institute of Advanced Energy, Kyoto University, Uji, Kyoto 611-0011, Japan; Present Address: Interdisciplinary Program of Biomedical Engineering, Assistive Technology, and Art and Sports Sciences, Faculty of Engineering, Niigata University, 8050 Ikarashi 2-no-cho, Nishi-ku, Niigata, 950-2181, Japan

Satoshi Yasuda – Graduate School of Science and Membrane Protein Research and Molecular Chirality Research Centers, Chiba University, Chiba 263-8522, Japan; orcid.org/0000-0003-3555-1083

Atsushi P. Kimura – Faculty of Science and Graduate School of Life Science, Hokkaido University, Sapporo 060-0810, Japan

Masahiro Kinoshita – Institute of Advanced Energy, Kyoto University, Uji, Kyoto 611-0011, Japan; Graduate School of Science and Membrane Protein Research and Molecular Chirality Research Centers, Chiba University, Chiba 263-8522, Japan; orcid.org/0000-0001-8060-045X

Takeshi Murata – Graduate School of Science and Membrane Protein Research and Molecular Chirality Research Centers, Chiba University, Chiba 263-8522, Japan

Kazuki Sada – Faculty of Science and Graduate School of Chemical Sciences and Engineering, Hokkaido University, Sapporo 060-0810, Japan; orcid.org/0000-0001-7348-0533

Complete contact information is available at: <https://pubs.acs.org/10.1021/acsomega.1c06699>

Author Contributions

^VA.R.M.K. and T. Munmun contributed equally to this work.

Author Contributions

Conceptualization was done by A.M.R.K.; funding acquisition was done by A.M.R.K., A.K., and T. Murata; development and validation of methodology was done by T. Munmun and A.M.R.K.; materials preparation was done by A.M.R.K., T. Munmun, T.H., S.Y., A.P.K., M.K., T. Murata, and A.K.; investigation was done by T. Munmun and A.M.R.K.; data analysis was done by T. Munmun; project administration and supervision were done by A.M.R.K.; original draft writing was done by A.M.R.K. and T. Munmun; review and editing of the manuscript were done by A.M.R.K., T. Munmun, T.H., S.Y., A.P.K., M.K., T. Murata, K.S., and A.K.

Notes

The authors declare no competing financial interest.

ACKNOWLEDGMENTS

This work was supported by a research grant (PK22201017) from Hirose Foundation and JSPS KAKENHI grant numbers JP21K04846 and JP20H05972 awarded to A.M.R.K.; JSPS KAKENHI grant numbers JP18H05423, JP21H04434, and JP21K19877 awarded to A. K.; and JSPS KAKENHI grant number JP18H05425 awarded to T. Murata.

REFERENCES

- (1) Howard, J. *Mechanics of motor protein and cytoskeleton*. Sinauer Associates Inc., 2001.
- (2) Yildiz, A.; Tomishige, M.; Vale, R. D.; Selvin, P. R. Kinesin walks hand-over-hand. *Science* **2004**, *303*, 676–678.
- (3) Van den Heuvel, M. G.; Dekker, C. Motor proteins at work for nanotechnology. *Science* **2007**, *317*, 333–336.
- (4) Jia, Y.; Li, J. Molecular assembly of rotary and linear motor proteins. *Acc. Chem. Res.* **2019**, *52*, 1623–1631.
- (5) Hess, H. Engineering applications of biomolecular motors. *Annu. Rev. Biomed. Eng.* **2011**, *13*, 429–450.
- (6) Bachand, G. D.; Rivera, S. B.; Boal, A. K.; Gaudio, J.; Liu, J.; Bunker, B. C. Assembly and transport of nanocrystal CdSe quantum dot nanocomposites using microtubules and kinesin motor proteins. *Nano Lett.* **2004**, *4*, 817–821.
- (7) Bachand, G. D.; Rivera, S. B.; Carroll-Portillo, A.; Hess, H.; Bachand, M. Active capture and transport of virus particles using a biomolecular motor-driven, nanoscale antibody sandwich assay. *Small* **2006**, *2*, 381–385.
- (8) Hess, H.; Clemmens, J.; Howard, J.; Vogel, V. Surface imaging by self-propelled nanoscale probes. *Nano Lett.* **2002**, *2*, 113–116.
- (9) Inoue, D.; Nitta, T.; Kabir, A. M. R.; Sada, K.; Gong, J. P.; Konagaya, A.; Kakugo, A. Sensing surface mechanical deformation using active probes driven by motor proteins. *Nat. Commun.* **2016**, *7*, 12557.
- (10) Hess, H.; Howard, J.; Vogel, V. A piconewton force meter assembled from microtubules and kinesins. *Nano Lett.* **2002**, *2*, 1113–1115.
- (11) Keya, J. J.; Kabir, A. M. R.; Inoue, D.; Sada, K.; Hess, H.; Kuzuya, A.; Kakugo, A. Control of swarming of molecular robots. *Sci. Rep.* **2018**, *8*, 11756.
- (12) Kabir, A. M. R.; Inoue, D.; Kakugo, A. Molecular swarm robots: recent progress and future challenges. *Sci. Technol. Adv. Mater.* **2020**, *21*, 323–332.
- (13) Nicolau, D. V., Jr.; Lard, M.; Korten, T.; van Delft, F. C. M. J. M.; Persson, M.; Bengtsson, E.; Månsson, A.; Diez, S.; Linke, H. Parallel computation with molecular-motor-propelled agents in

- nanofabricated networks. *Proc. Natl. Acad. Sci. U. S. A.* **2016**, *113*, 2591–2596.
- (14) Matsuda, K.; Kabir, A. M. R.; Akamatsu, N.; Saito, A.; Ishikawa, S.; Matsuyama, T.; Ditzer, O.; Islam, M. S.; Ohya, Y.; Saka, K.; Konagaya, A.; Kuzuya, A.; Kakugo, A. Artificial smooth muscle model composed of hierarchically ordered microtubule asters mediated by DNA origami nanostructures. *Nano Lett.* **2019**, *19*, 3933–3938.
- (15) Isozaki, N.; Shintaku, H.; Kotera, H.; Hawkins, T. L.; Ross, J. L.; Yokokawa, R. Control of molecular shuttles by designing electrical and mechanical properties of microtubules. *Sci. Robot.* **2017**, *2*, No. aan4882.
- (16) Keya, J. J.; Suzuki, R.; Kabir, A. M. R.; Inoue, D.; Asanuma, H.; Sada, K.; Hess, H.; Kuzuya, A.; Kakugo, A. DNA-assisted swarm control in a biomolecular motor system. *Nat. Commun.* **2018**, *9*, 453.
- (17) Wada, S.; Kabir, A. M. R.; Ito, M.; Inoue, D.; Sada, K.; Kakugo, A. Effect of length and rigidity of microtubules on the size of ring-shaped assemblies obtained through active self-organization. *Soft Matter* **2015**, *11*, 1151–1157.
- (18) Kawamura, R.; Kakugo, A.; Osada, Y.; Gong, J. P. Selective formation of a linear-shaped bundle of microtubules. *Langmuir* **2010**, *26*, 533–537.
- (19) Akter, M.; Keya, J. J.; Kabir, A. M. R.; Asanuma, H.; Murayama, K.; Sada, K.; Kakugo, A. Photo-regulated trajectories of gliding microtubules conjugated with DNA. *Chem. Commun.* **2020**, *56*, 7953–7956.
- (20) Mickey, B.; Howard, J. Rigidity of microtubules is increased by stabilizing agents. *J. Cell Biol.* **1995**, *130*, 909–917.
- (21) Inaba, H.; Yamamoto, T.; Iwasaki, T.; Kabir, A. M. R.; Kakugo, A.; Sada, K.; Matsuura, K. Stabilization of microtubules by encapsulation of the GFP using a Tau-derived peptide. *Chem. Commun.* **2019**, *55*, 9072–9075.
- (22) Kelly, R. H.; Yancey, P. H. High contents of trimethylamine oxide correlating with depth in deep-sea teleost fishes, skates, and decapod crustaceans. *Biol. Bull.* **1999**, *196*, 18–25.
- (23) Yancey, P. H.; Clark, M. E.; Hand, S. C.; Bowlus, R. D.; Somero, G. N. Living with water stress: evolution of osmolyte systems. *Science* **1982**, *217*, 1214–1222.
- (24) Chase, K.; Doval, F.; Vershinin, M. Enhanced stability of kinesin-I as a function of temperature. *Biochem. Biophys. Res. Commun.* **2017**, *493*, 1318–1321.
- (25) Munmun, T.; Kabir, A. M. R.; Katsumoto, Y.; Sada, K.; Kakugo, A. Controlling the kinetics of interaction between microtubules and kinesins over a wide temperature range using the deep-sea osmolyte trimethylamine N-oxide. *Chem. Commun.* **2020**, *56*, 1187–1190.
- (26) Munmun, T.; Kabir, A. M. R.; Sada, K.; Kakugo, A. Complete, rapid and reversible regulation of the motility of a nano-biomolecular machine using an osmolyte trimethylamine-N-oxide. *Sens. Actuators B Chem.* **2020**, *304*, 127231.
- (27) Kumemoto, R.; Yusa, K.; Shibayama, T.; Hatori, K. Trimethylamine N-oxide suppresses the activity of the actomyosin motor. *Biochim. Biophys. Acta Gen. Subj.* **2012**, *1820*, 1597–1604.
- (28) VanDelinder, V.; Sickafoose, I.; Imam, Z. I.; Ko, R.; Bachand, G. D. The effects of osmolytes on in vitro kinesin-microtubule motility assays. *RSC Adv.* **2020**, *10*, 42810–42815.
- (29) Wisanpitayakorn, P.; Mickolajczyk, K. J.; Hancock, W. O.; Vidali, L.; Tüzel, E. Measurement of the persistence length of cytoskeletal filaments using curvature distributions. *Preprint at bioRxiv* **2018**, 252551.
- (30) Bachand, G. D.; Jain, R.; Ko, R.; Bouxsein, N. F.; VanDelinder, V. Inhibition of microtubule depolymerization by osmolytes. *Biomacromolecules* **2018**, *19*, 2401–2408.
- (31) Rupp, B.; Nédélec, F. Patterns of molecular motors that guide and sort filaments. *Lab Chip* **2012**, *12*, 4903–4910.
- (32) Pampaloni, F.; Lattanzi, G.; Jonáš, A.; Surrey, T.; Frey, E.; Florin, E. L. Thermal fluctuations of grafted microtubules provide evidence of a length-dependent persistence length. *Proc. Natl. Acad. Sci. U. S. A.* **2006**, *103*, 10248–10253.
- (33) Zhou, H.; Isozaki, N.; Fujimoto, K.; Yokokawa, R. Growth rate-dependent flexural rigidity of microtubules influences pattern formation in collective motion. *J. Nanobiotechnology* **2021**, *19*, 218.
- (34) Kabir, A. M. R.; Inoue, D.; Hamano, Y.; Mayama, H.; Sada, K.; Kakugo, A. Biomolecular motor modulates mechanical property of microtubule. *Biomacromolecules* **2014**, *15*, 1797–1805.
- (35) Ma, J.; Pazos, I. M.; Gai, F. Microscopic insights into the protein-stabilizing effect of trimethylamine N-oxide (TMAO). *Proc. Natl. Acad. Sci. U. S. A.* **2014**, *11*, 8476–8481.
- (36) Zou, Q.; Bennion, B. J.; Daggett, V.; Murphy, K. P. The molecular mechanism of stabilization of proteins by TMAO and its ability to counteract the effects of urea. *J. Am. Chem. Soc.* **2002**, *124*, 1192–1202.
- (37) Sackett, D. L. Natural osmolyte trimethylamine N-oxide stimulates tubulin polymerization and reverses urea inhibition. *Am. J. Physiol. Regul. Integr. Comp. Physiol.* **1997**, *273*, R669–R676.
- (38) Yancey, P. H. *Water and Life*. Edited by Somero, G. N.; Osmond, C. B.; Bolis, C. L. New York: Springer, Berlin, Heidelberg, 1992; pp. 19–32.
- (39) Saper, G.; Hess, H. Synthetic systems powered by biological molecular motors. *Chem. Rev.* **2019**, *120*, 288–309.
- (40) Zeisel, S. H.; Warrier, M. Trimethylamine N-Oxide, the microbiome, and heart and kidney disease. *Annu. Rev. Nutr.* **2017**, *37*, 157–181.
- (41) Castoldi, M.; Popov, A. V. Purification of brain tubulin through two cycles of polymerization–depolymerization in a high-molarity buffer. *Protein Expression Purif.* **2003**, *32*, 83–88.
- (42) Peloquin, J.; Komarova, Y.; Borisy, G. Conjugation of fluorophores to tubulin. *Nat. Methods* **2005**, *2*, 299–303.
- (43) Fujimoto, K.; Kitamura, M.; Yokokawa, M.; Kanno, I.; Kotera, H.; Yokokawa, R. Colocalization of quantum dots by reactive molecules carried by motor proteins on polarized microtubule arrays. *ACS Nano* **2012**, *7*, 447–455.
- (44) Arii, Y.; Hatori, K. Relationship between the flexibility and the motility of actin filaments: effects of pH. *Biochem. Biophys. Res. Commun.* **2008**, *371*, 772–776.
- (45) Kabir, A. M. R.; Wada, S.; Inoue, D.; Tamura, Y.; Kajihara, T.; Mayama, H.; Sada, K.; Kakugo, A.; Gong, J. P. Formation of ring-shaped assembly of microtubules with a narrow size distribution at an air-buffer interface. *Soft Matter* **2012**, *8*, 10863–10867.